# HYPERSPECTRAL UAS IMAGERY FOR GRASS SWARDS BIOMASS AND NITROGEN ESTIMATION

R. A. Oliveira [1]*, R. Näsi [1], P. Korhonen [2], A. Mustonen [2], O. Niemeläinen [2], N. Koivumäki[1], T. Hakala [1], J. Suomalainen [1], J. Kaivosoja [2], E. Honkavaara [1]

[1] Dept. of Remote Sensing and Photogrammetry, Finnish Geospatial Research Institute of National Land Survey of Finland, Vuorimehentie, 02150, Espoo, Finland - (raquel.alvesdeoliveira, roope.nasi, niko.koivumaki, teemu.hakala, juha.suomalaine, eija.honkavaara)@nls.fi

[2] Natural Resources Institute Finland (Luke), Finland – (panu.korhonen, arja.mustonen, oiva.niemelainen, jere.kaivosoja)@luke.fi

**KEY WORDS:** Hyperspectral, Unmanned Aerial System (UAS), Grass Biomass, Nitrogen Concentration, Machine Learning.

**ABSTRACT:**

Monitoring agricultural grass fields is particularly important for meat and milk production in Northern Europe, where three harvests occur during a growing season to maximize yields. Reliable data on forage, including biomass and nitrogen concentration, are essential for making informed decisions regarding seed mixtures, fertilizer rates, and harvest timing. Miniaturized hyperspectral cameras mounted on unmanned aerial systems (UAS) have become increasingly accessible and efficient. These cameras, operating in the visible to near-infrared (VNIR) range, have shown potential in estimating grass sward quantity and feeding quality. Additional advancements in hyperspectral technology have emerged the short-wave infrared (SWIR) range for UAS applications, previously utilized mainly in laboratory and aircraft-based systems. This study aims to explore the potential of VNIR and SWIR hyperspectral UAS-based remote sensing in biomass and nitrogen estimation during primary and re-growth stages. Grass fresh yield and nitrogen concentration prediction models were built after selecting the most significant features from the cameras to cope with the high dimensionality of the data. Using best features and machine learning, both fresh yield and nitrogen concentration were estimated with normalized root mean square error better than 10%. This work contributes to the development of accurate remote sensing techniques, supporting sustainable agricultural practices and climate change studies.

## 1. INTRODUCTION

Closely monitoring agricultural grassland fields plays a critical role in fostering sustainable planning and effective resource management, key components of climate change studies. The implementation of efficient and sustainable practices is vital to prevent substantial environmental losses and mitigate biodiversity degradation resulting from agricultural expansion (Himanen et al., 2016). Accurate data on forage, encompassing biomass levels and nitrogen concentration, are of greatest importance when making decisions about seed mixtures, fertilizer application rates, and the optimal timing for harvesting. Grass silage is essential for ruminant meat and milk production in Northern Europe, where the grass is usually harvested three times in a growing season to maximise the yield.

The advent of miniaturized hyperspectral cameras that can be mounted on unoccupied aerial systems (UAS) has become more efficient and accessible. RGB imaging has been the most common UAS-based method to estimate above-ground biomass (Bazzo et al. 2023). However, the multispectral cameras have been adopted to estimate grass properties as well (e.g. Askari et al. 2019; Lussem et al. 2022; Viljanen et al. 2018). The potential of UAV-based hyperspectral cameras operated in visible to near-infrared (VNIR) to estimate quantity and feeding quality of grass swards has been investigated in several studies (Wijesinghha et al. 2020, Oliveira et al. 2020, and Karila et al., 2022).

While most UAS remote sensing cameras currently operate within the VNIR spectral range (400-900 nm), recent advancements have made hyperspectral short-wave infrared (SWIR) range viable for UAS applications. Traditionally, SWIR range was mainly used for laboratory-based analysis using techniques such as near-infrared spectroscopy (NIRS) or field spectroscopy (Togeiro de Alckmin et al., 2020, Fernández-Habas et al 2022, and Pullanagari et al., 2021), as well as using aircraft-based systems.

Investigating the potential of both the VNIR and SWIR ranges is particularly important as it can provide valuable information on the spectral characteristics of grass for silage. Understanding these characteristics can enable the development of more targeted and accurate remote sensing techniques, allowing for precise estimation of yield and nitrogen levels. Furthermore, advancements in hyperspectral technology and ongoing research efforts are expected to contribute to the increased accessibility of these sensors in the future, provide insights for the development of new sensors and improved algorithms, opening new opportunities for their widespread adoption in precision agriculture applications.

Jenal et al. (2020) has investigated an in-house multispectral VNIR/SWIR camera with four bands for grass biomass estimation. They verify that the camera had potential in the application, but more studies are needed considering a wider spectral range, other parameters, and more growth periods. Recently, Oliveira et al. (2023) investigated for the first time the potential of drone-based hyperspectral SWIR sensor in various grass parameters estimation task and compared its performance to hyperspectral VNIR, multispectral and RGB UAS remote sensing. They concluded that generally hyperspectral datasets and combination of them provided the best results, whereas the


https://doi.org/10.5194/isprs-archives-XLVIII-1-W2-2023-1861-2023  

worst accuracies were obtained using the RGB data. However, in Oliveira et al. (2023), only one dataset from re-growth (third cut) was used and as grass properties can be different for primary growth (first cut), it is important to study if similar conclusions can be drawn also in other growing conditions.

The main aim of this work is to investigate the potential of hyperspectral UAS-based Remote Sensing sensors in biomass and nitrogen estimation of grass sward during primary and re-growth, by identifying and analysing specific spectral ranges of each hyperspectral cameras. Two novel hyperspectral cameras operating in the VNIR and SWIR ranges were employed to collect data over grass swards for two different grows of consecutive years. A machine learning framework was utilized to estimate the grass parameters, and both cameras were employed independently as well as through data fusion.

## 2. MATERIALS AND METHODS

### 2.1 Experimental design and field data

The experimental trial was established by the Natural Resources Institute Finland (Luke) in Maaninka, Finland. The experiment was designed with a total of 60 grass plots, including four replicates, three main plots and five subplots (total nitrogen 0, 150, 250, 350 or 450 kg N $ha^{-1}$ $year^{-1}$). The plot dimensions were 1.5 m x 8 m and each plot was separated by a similar sized cover plot. The plant material was pure timothy (*Phleum pratense* L). The agronomic details of experiment can be found from Termonen et al. (2022)

The trial was maintained in similar conditions in 2021 (See more details in Oliveira et al. 2023) and 2022. In this study, two cuts of grass data were used, which were collected in the third harvest of 2021 and the first harvest of 2022. The field sampling data measurements of the plots analysed in this study were fresh yield (FY) and nitrogen concentration (Ncont). Table 1 shows mean and standard deviation, minimum and maximum values of field measurements for each parameter. FY and Ncont range were highest in the first cut of 2022.

| Data | Mean | Std | Min | Max |
|---|---|---|---|---|
| Third cut 2021 FY (kg $ha^{-1}$) | 8424 | 3825 | 375 | 13858 |
| First cut 2022 FY (kg $ha^{-1}$) | 21947 | 4749 | 6750 | 28417 |
| Third cut 2021 Ncont (%) | 2.7 | 0.4 | 2.1 | 3.5 |
| First cut 2022 Ncont (%) | 2.5 | 0.5 | 1.6 | 3.2 |

**Table 1**: Third cut of 2021 and first cut of 2022 timothy data mean, standard deviation (Std), minimum (Min), and maximum (Max). FY: fresh yield; Ncont: nitrogen concentration.

### 2.2 Hyperspectral UAS imagery data

The hyperspectral UAS data collection was carried out in August 2021, in the third harvesting, and in June 2022 using two pushbroom hyperspectral cameras by Specim. AFX10 camera operates in 400–1000 nm (VNIR) and has 2.1 kg and had a spectral resolution of 5.5 nm, a spectral sampling of 2.68 nm, spectral binning of 2, 224 bands, 1024 spatial pixels and focal length 15 mm. The AFX17 camera operates in 900–1700 nm (SWIR) range (2.4 kg, no spectral binning) had a spectral resolution of 8 nm, a spectral sampling of 3.5 nm, 224 bands, 640 spatial pixels, and a focal length of 18 mm (Specim, 2023). The flights were conducted from approximately 100 m above ground level, with same trajectory using one camera at a time, each mounted on a DJI Matrice 600. In 2021, the flights were carried out 26 August 2021 and, in 2022, the flights with AFX17 (SWIR) and AFX10 (VNIR) were done on 13 June and 15 June, respectively.

The raw image pixel values of AFX datasets were transformed to the units of radiance using the Specim CaliGeoPRO v2.3.12 software. The AFX10 datasets from both years were collected under uniform conditions, whereas the AFX17 datasets was collected under in varying conditions. The datasets of 2022 had slight worse orthorectification quality due to technical issues on the cameras GNSS/IMU and gimbal. The reflectance transformation was performed using empirical line method with four reflectance reference panels of 1 m × 1 m size and nominal reflectance equal to 50%, 25%, 10%, and 5%, for 2021 datasets, and two panels (50% and 5%) for 2022 datasets. Figure 1 shows the orthomosaic of AFX10 camera for each dataset.

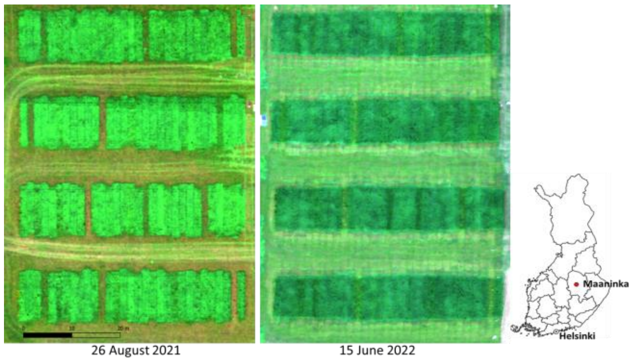


**Figure 1**. VNIR (AFX10) orthomosaics for third cut of 2021 and first cut of 2022.

### 2.3 Correlation analysis and grass parameter estimation

The estimation process involved three main steps: feature extraction, feature selection, and supervised learning. Several spectral features were extracted from each camera reflectance orthomosaic for each grass plot (8 m x 1 m). Spectral related statistics features were 1,880 features, for VNIR, 1750 features, for SWIR (see Nevalainen et al. 2017). Besides, simple band ratio (SBR) of the reflectance spectra (Chappelle et al., 1992) and two-band normalised difference (NBR) (Thenkabail et al., 2013) were computed to for all band combinations. This resulted in 17578 combinations for VNIR and 15225 combinations for SWIR. After feature extraction, relationship between individual features and grass parameters were analysed and Pearson correlation coefficient (PCC) was used as a metric.

To refine the feature set, a recursive feature selection cross-validation (RFECV) method was used, implemented in Scikit-learn, with 10-fold cross-validation based on the random forest (RF) estimator's importance. Random Forest is a supervised machine learning algorithm. During the RFECV process, the feature importance starting with all features, and then iteratively dropping one or a few features until the minimum number of features (limited to 40) was reached. The final set of selected features was chosen based on the mean results from the different splits, and the best scored iteration was selected. The selected features were used to create RF FY and Ncont prediction models. The accuracy of the models was assessed through leave one out cross validation (LOOCV).


https://doi.org/10.5194/isprs-archives-XLVIII-1-W2-2023-1861-2023  

The performance of the hyperspectral data was tested by building models VNIR dataset and SWIR dataset and by combining both features dataset (VNIR-SWIR). Besides, each cut was predicted independently and combined.

## 3. RESULTS AND DISCUSSION

### 3.1 Fresh yield

The PCC values between FY and several spectral bands were higher for the third cut 2021 than for first cut 2022. The best PCCs where found in range 745 nm – 1300 nm for both FY (Figure 2). Interestingly, the PCCs between FY and bands from green area (550 nm) were relatively high (0.86) in re-growth (third cut) dataset in comparison to first cut dataset from 2022 (0.2). Furthermore, in area in range 1500 – 1700 nm the PCC varied more in third cut dataset (0.28-0.88) than in first cut dataset (0.65-0.75)

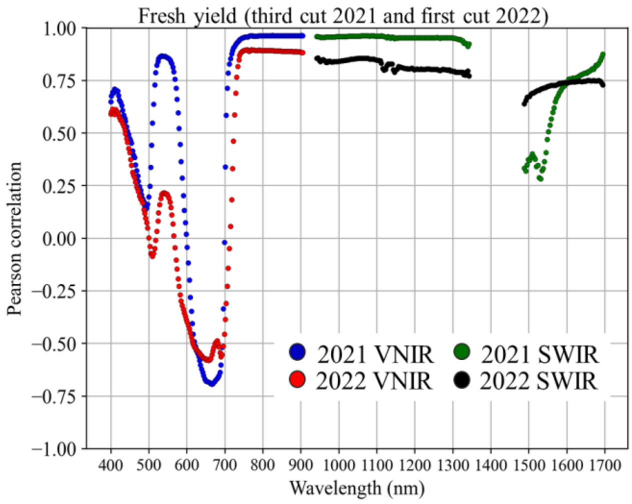


**Figure 2**. The Pearson correlation coefficients (PCC) for individual bands of VNIR and SWIR cameras and fresh yield (FY), in third cut of 2021 and third cut of 2022.

Normalized band ratio indices among each camera band also presented high correlations for both VNIR and SWIR cameras, with PCCs of -0.98 (Figure 3). Band ratio indices draw relatively similar figure for VNIR sensor in both datasets but SWIR sensor some changes were visible. For instance, the band ratios created from bands from 1500-1700 nm showed positive PCC for third cut data but for the first cut the PCC were small and mainly negative. The relationship is in line with earlier experiments using ground spectrometers (for example Psomas et al. 2011)

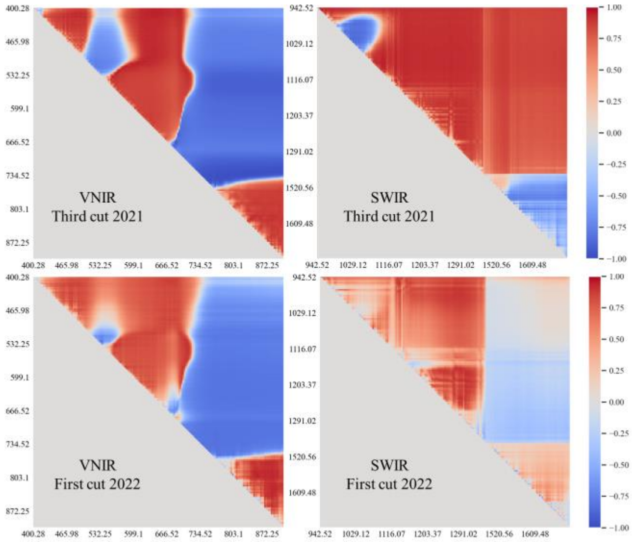


**Figure 3.** Pearson correlation coefficients (PCC) for Normalized band ratio indices of VNIR and SWIR cameras and fresh yield (FY), in third cut of 2021 and first cut of 2022.

Table 2 presents the RMSE and NRMSE and $R^2$ resulting from the LOOCV for FY estimation, organised by sensor and sensors, and it shows results for each cut separately as well as for both cuts combined in the estimation dataset.

Considering the estimation for the third cut of 2021, the features from VNIR-SWIR achieved the best performance (NRMSE 8.42%), while the results from using only VNIR and SWIR were comparable (VNIR: NRMSE 9.59% and SWIR: NRMSE 9.29%). This reflects the high correlation levels noticed in both VNIR and SWIR (Figure 2).

For first cut of 2022, the fusion of VNIR-SWIR (NRMSE 6.15%) and VNIR (NRMSE 6.64%) had similar performance and better results than the estimation using only SWIR features (NRMSE 8.28%).

Comparing both cuts' results, the third cut obtained best absolute accuracies as the RMSEs were smaller than for the first cut, but worse relative accuracy (higher NMSEs). This is likely related to the lower variation and range of the third cut training dataset (see Table 1).

The combination of the different cuts presented best NRMSE of 10.33% and RMSE 1563 kg $ha^{-1}$, obtained by VNIR-SWIR. Although, the model had not improved the accuracy when using two cuts, the datasets present a relatively good degree of fit (Figure 4).

| Fresh Yield | | | | |
|---|---|---|---|---|
| **Data** | **Feature group** | **RMSE (kg DM ha$^{-1}$)** | **NRMSE (%)** | **$R^2$** |
| **3rd cut 2021** | VNIR | 808 | 9.59 | 0.96 |
| | SWIR | 779 | 9.25 | 0.96 |
| | VNIR-SWIR | 709 | 8.42 | 0.97 |
| **1st cut 2022** | VNIR | 1457 | 6.64 | 0.90 |
| | SWIR | 1816 | 8.28 | 0.85 |
| | VNIR-SWIR | 1350 | 6.15 | 0.92 |
| **3rd cut 2021 and 1st cut 2022** | VNIR | 1630 | 10.77 | 0.96 |
| | SWIR | 1666 | 11.01 | 0.96 |
| | VNIR-SWIR | 1563 | 10.33 | 0.96 |

**Table 2**: Fresh yield leave-one out cross validation using third cut of 2021 and first cut of 2022. RMSE: root mean square error, NRMSE: normalized RMSE and $R^2$: coefficient of determination.

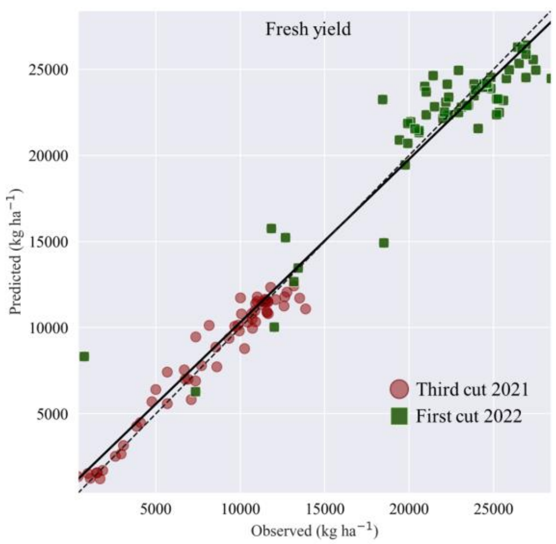


**Figure 4.** The relationship between the predicted and observed values for the fresh yield (FY) (LOOCV – Leave-one-out cross validation) using VNIR and SWIR features combined, in third cut of 2021 and first cut of 2022.

### 3.2 Nitrogen concentration

PCC values for Ncont were higher for first cut 2022, mainly in the wavelengths between 400 and 500 nm and 700 and 800 nm, which are recognized for their sensitivity to nitrogen (Figure 5). Overall, PCCs were lower for Ncont than for FY, with values slightly over 0.65 for in spectral ranges 770 nm – 1335nm and 1670 nm – 1695 nm (Figure 5). Similarly, to FY (Figure 2) the correlation between in bands from green area and Ncont was higher in the third cut data than in first cut dataset. The normalized band ratios of the VNIR camera presented higher PCCs values (maximum PCC 0.76) than the SWIR normalized ratios (maximum PCC 0.64) (Figure 6).

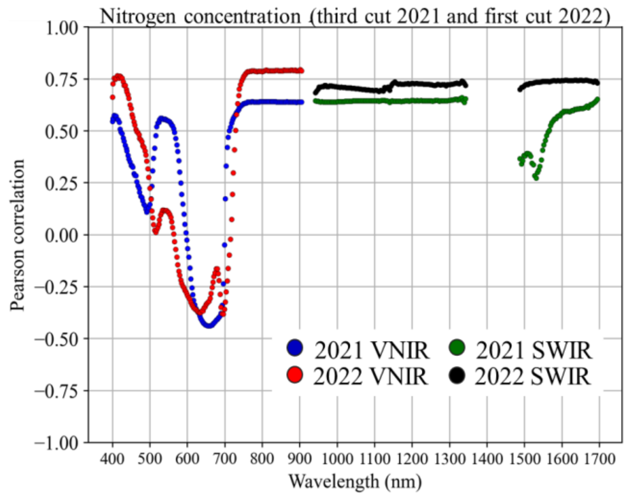


**Figure 5**. The Pearson correlation coefficients (PCC) for individual bands of VNIR and SWIR cameras and nitrogen concentration (Ncont), in third cut of 2021 and third cut of 2022.

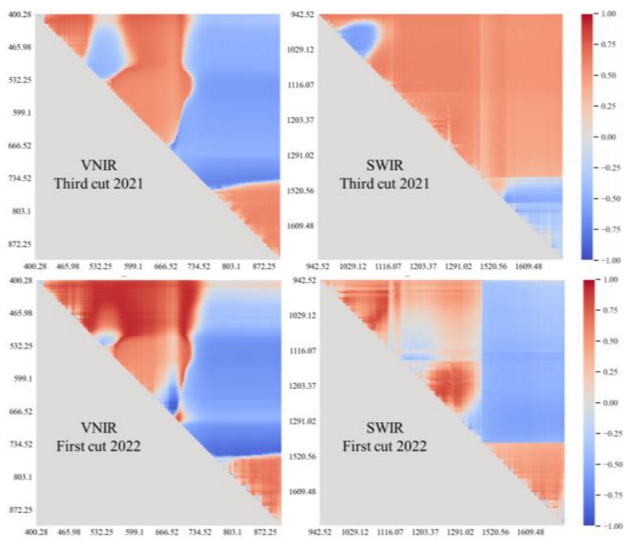


**Figure 6.** Pearson correlation coefficients (PCC) for Normalized band ratio indices of VNIR and SWIR cameras and nitrogen concentration in third cut of 2021 and first cut of 2022.

Overall, the results for Ncont estimation (Table 3) of the third cut of 2021 were similar. At the best NRMSE 8.04% and RMSE 0.22% using only VNIR features. VNIR_SWIR dataset presented slightly higher NRMSE 8.62% and RMSE 0.23% and SWIR alone obtained NRMSE 9.01% and RMSE 0.24%.

The first cut of 2022 estimation outperformed the results of the third cut 2021. As expected, based on the higher PCCs of VNIR range with Ncont than the SWIR range (Figure 5), the VNIR dataset (NRMSE 5.4% and RMSE 0.13%) had clearly better accuracy than the SWIR (NRMSE 9.2% and RMSE 0.23%). Thus, the combination of VNIR and SWIR features did not improve the results obtained using only VNIR.

The results of the using third and first cuts combined slightly improved the third cut results but not the first cut. Combined model showed slightly overestimated values for low and underestimated values for samples with high nitrogen concentration (Figure 7).

| Nitrogen concentration | | | | |
|---|---|---|---|---|
| **Data** | **Feature group** | **RMSE** | **NRMSE (%)** | **$R^2$** |
| **3rd cut 2021** | VNIR | 0.22 | 8.04 | 0.65 |
| | SWIR | 0.24 | 9.01 | 0.56 |
| | VNIR_SWIR | 0.23 | 8.62 | 0.60 |
| **1st cut 2022** | VNIR | 0.13 | 5.40 | 0.92 |
| | SWIR | 0.23 | 9.20 | 0.76 |
| | VNIR_SWIR | 0.14 | 5.55 | 0.91 |
| **3rd cut 2021 and 1st cut 2022** | VNIR | 0.20 | 7.60 | 0.79 |
| | SWIR | 0.23 | 8.94 | 0.72 |
| | VNIR_SWIR | 0.20 | 7.54 | 0.80 |

**Table 3**: Nitrogen concentration leave-one out cross validation using third cut of 2021 and first cut of 2022. RMSE: root mean square error, NRMSE: normalized RMSE and $R^2$: coefficient of determination.

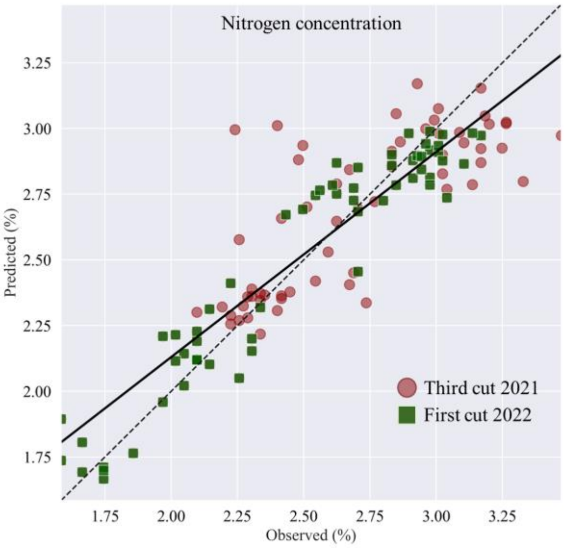


**Figure 7.** The relationship between the predicted and observed values for the nitrogen concentration (LOOCV – Leave-one-out cross validation) using VNIR and SWIR features combined, in third cut of 2021 and first cut of 2022.

## 4. CONCLUSIONS

This study investigated the potential of two new hyperspectral UAS-based Remote Sensing sensors operating in VNIR and SWIR spectral ranges in biomass and nitrogen estimation of grass sward during primary and re-growth, by identifying and analysing specific spectral ranges of each hyperspectral cameras. This study showed that ultra-high resolution hyperspectral sensors provide accurate data for biomass (fresh yield) and nitrogen concentration estimation in two different growing conditions. The VNIR outperformed SWIR camera for the first cut for both FY and Ncont, and slightly for the third cut. However, more studies are needed to build robust estimation models able to handle more challenging conditions, such as different growing conditions and mixed grass species.

## ACKNOWLEDGEMENTS

This research was funded by Academy of Finland ICT 2023 Smart-HSI - "Smart hyperspectral imaging solutions for new era in Earth and planetary observations" (Decision no. 335612), by the European Agricultural Fund for Rural Development: Europe investing in rural areas (North Savo ELY Centre) - "Remote sensing methods to support feed production REHUDROONI" (Grant no. 145346), by the European Regional Development Fund for "CyberGrass I - Introduction to remote sensing and artificial intelligence assisted silage production" project (ID 20302863) in the European Union Interreg Botnia-Atlantica programme, and by the Ministry of Agriculture and Forestry of Finland project NC Grass - Dairy and beef industries in Finland: Progressing pathways to carbon-neutrality by 2035 (VN/28562/2020-MMM-2). The field trial was funded mainly by the European Agricultural Fund for Rural Development ("Production Resilience from Grass - VarmaNurmi" project). This research was carried out in affiliation with the Academy of Finland Flagship "Forest-Human-Machine Interplay - Building Resilience, Redefining Value Networks and Enabling Meaningful Experiences (UNITE)" (Decision no. 337127) ecosystem.

## REFERENCES

Askari, M. S., McCarthy, T., Magee, A., & Murphy, D. J., 2019. Evaluation of grass quality under different soil management scenarios using remote sensing techniques. Remote Sensing, 11(15), 1835.

Bazzo, C. O. G., Kamali, B., Hütt, C., Bareth, G., & Gaiser, T., 2023. A review of estimation methods for aboveground biomass in grasslands using UAV. Remote Sensing, 15(3), 639.

Chappelle, Emmett W.; Kim, M.S.M.J.E., 1992. Ratio analysis of reflectance spectra (RARS): An algorithm for the remote estimation of the concentrations of chlorophyll a, chlorophyll b, and carotenoids in soybean leaves. Remote Sensing of Environment 39, 239–247, 10.1016/0034-4257(92)90089-3.

Fernández-Habas, J., Cañada, M.C., Moreno, A.M.G., Leal-Murillo, J.R., González-Dugo, M.P., Oar, B.A., Gómez-Giráldez, P.J., Fernández-Rebollo, P., 2022. Estimating pasture quality of mediterranean grasslands using hyperspectral narrow bands from field spectroscopy by random forest and PLS regressions. Computers and Electronics in Agriculture 192, 106614. https://doi.org/10.1016/j.compag.2021.106614

Himanen, S. J., Mäkinen, H., Rimhanen, K., & Savikko, R. (2016). Engaging farmers in climate change adaptation planning: Assessing intercropping as a means to support farm adaptive capacity. Agriculture, 6(3), 34.

Jenal, A., Lussem, U., Bolten, A., Gnyp, M.L., Schellberg, J., Jasper, J., Bongartz, J., Bareth, G., 2020. Investigating the potential of a newly developed UAV-based VNIR/SWIR imaging system for forage mass monitoring. PFG–Journal of Photogrammetry, Remote Sensing and Geoinformation Science 88, 493–507.

Karila, K., Oliveira, R.A., Ek, J., Kaivosoja, J., Koivumäki, N., Korhonen, P., Niemeläinen, O., Nyholm, L., Näsi, R., Pölönen, I., et al., 2022. Estimating grass sward quality and quantity parameters using drone remote sensing with deep neural networks. Remote Sensing 14, 2692.

Lussem, U., Bolten, A., Kleppert, I., Jasper, J., Gnyp, M. L., Schellberg, J., & Bareth, G., 2022. Herbage Mass, N Concentration, and N Uptake of Temperate Grasslands Can Adequately Be Estimated from UAV-Based Image Data Using Machine Learning. Remote Sensing, 14(13), 3066.

Nevalainen, O., Honkavaara, E., Tuominen, S., Viljanen, N., Hakala, T., Yu, X., Hyyppä, J., Saari, H., Pölönen, I., Imai, N.N., et al., 2017. Individual tree detection and classification with UAV-based photogrammetric point clouds and hyperspectral imaging. Remote Sensing 9, 185.

Oliveira, R.A., Näsi, R., Niemeläinen, O., Nyholm, L., Alhonoja, K., Kaivosoja, J., Jauhiainen, L., Viljanen, N., Nezami, S., Markelin, L., Hakala, T., Honkavaara, E., 2020. Machine learning estimators for the quantity and quality of grass swards used for silage production using dronebased imaging spectrometry and photogrammetry. Remote Sensing of Environment 246, 111830. https://doi.org/10.1016/j.rse.2020.111830 .

Oliveira, R.A., Näsi, R., Korhonen, P., Mustonen, A., Niemeläinen, O., Koivumäki, N., Hakala, T., Suomalainen, J., Kaivosoja, J., Honkavaara, E., 2023. High-precision estimation of grass quality and quantity using UAS-based VNIR and SWIR hyperspectral cameras and machine learning. Precision Agriculture. Springer.

Psomas, A., Kneubühler, M., Huber, S., Itten, K., & Zimmermann, N. E. 2011. Hyperspectral remote sensing for estimating aboveground biomass and for exploring species richness patterns of grassland habitats. International Journal of Remote Sensing, 32(24), 9007-9031.

Pullanagari, R., Dehghan-Shoar, M., Yule, I.J., Bhatia, N., 2021. Field spectroscopy of canopy nitrogen concentration in temperate grasslands using a convolutional neural network. Remote Sensing of Environment 257, 112353, https://doi.org/10.1016/j.rse.2021.112353.

Specim Spectral Imaging Ltd. 2022. Specim FX Series. Specim AFX Series. Available online: https://www.specim.fi/afx/ (accessed on 2 June 2023).

Termonen, M., Kykkänen, S., P., K., Mustonen, A., Seppänen, M., Virkajärvi, P., 2022. Combination of cattle slurry and mineral n fertilizer for efficient grass production in Finland. Proceedings of the 29th General Meeting of the European Grassland Federation Caen, France, Grassland at the heart of circular and sustainable food systems 27, 737–739.

Thenkabail, P.S., Mariotto, I., Gumma, M.K., Middleton, E.M., Landis, D.R., Huemmrich, K.F., 2013. Selection of Hyperspectral Narrowbands (HNBs) and Composition of Hyperspectral Twoband Vegetation Indices (HVIs) for Biophysical Characterization and Discrimination of Crop Types Using Field Reflectance and Hyperion/EO-1 Data. IEEE Journal of Selected Topics in Applied Earth Observations and Remote Sensing 6, 427–439, doi.org/10.1109/JSTARS.2013.2252601.

Viljanen, N.; Honkavaara, E.; Näsi, R.; Hakala, T.; Niemeläinen, O.; Kaivosoja, J. A novel machine learning method for estimating biomass of grass swards using a photogrammetric canopy height model, images and vegetation indices captured by a drone. Agriculture 2018, 8, 70.

Wijesingha, J., Astor, T., Schulze-Brüninghoff, D., Wengert, M., Wachendorf, M., 2020. Predicting forage quality of grasslands using uav-borne imaging spectroscopy. Remote Sensing 12, 126, https://doi.org/10.3390/rs12010126 .